Chemical and Biological Technologies in Agriculture

RESEARCH

Open Access

JUNB affects hair follicle development and regeneration by promoting the proliferation of dermal papilla cells in goat

Tongtong Zhang[1], Fang Li[1], Xiang Li[1], Xiongbo Zhou[1], Yujie Zheng[1] and Xin Wang[1*]

Abstract

Background The process of hair follicle morphogenesis, development, and regeneration essentially depends on the interaction between skin epidermis and dermis, while dermal papilla (DP) cells play a vital role in this process. Transcription factors recognize specific DNA sequences to regulate gene transcription during hair follicle development. Our previous sequencing data have demonstrated that JUNB is differentially expressed between the induction and differentiation stages during hair follicle development of cashmere goat. However, the underlying mechanism of JUNB currently remains unknown.

Results The function of *JUNB* on DP cells was explored by EdU, MTT, CCK-8, and flow cytometry analysis, which showed that JUNB significantly promoted the cell viability and proliferation. Subsequently, the underlying regulation mechanism of JUNB was investigated. The dual-luciferase reporter assay and RT-qPCR results revealed that *TCF3* was a target gene of JUNB. And the expressions of Wnt signaling pathway-related genes, *CTNNB1* (β-catenin), *Cyclin D1*, and *C-myc*, were significantly promoted at mRNA and protein levels. The homology analysis based on JUNB protein sequences revealed that goat and mouse had high homology among 11 species. Therefore, C57 BL/6 mice were selected as the animal model for further in vivo experiment. The result showed that *JUNB* promoted hair regeneration of mouse, and the HE and immunofluorescence staining results of skin tissues further proved it.

Conclusions Taken together, our results revealed that *JUNB* promoted the proliferation of DP cells by regulating Wnt signaling pathway, thereby affecting hair regeneration, which would provide molecular target for improving cashmere quality and breeding of cashmere goats.

Keywords Transcription factor JUNB, Hair follicle, DP cells, *TCF3*, Wnt signaling pathway

*Correspondence:
Xin Wang
xinwang5@nwsuaf.edu.cn
Full list of author information is available at the end of the article

Graphical Abstract

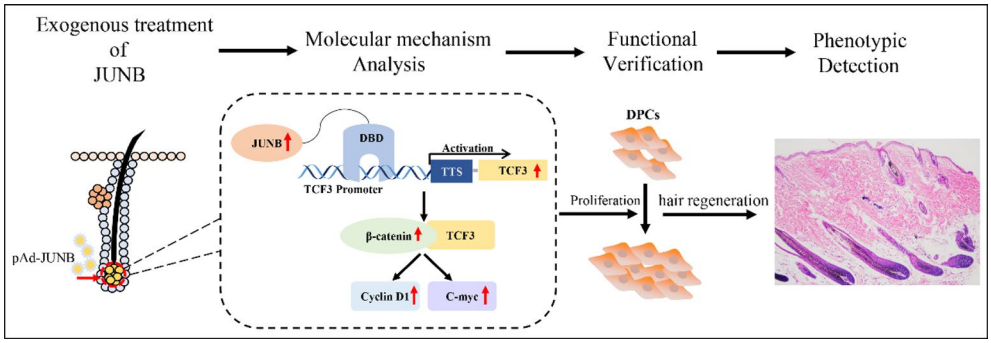

Introduction

Hair follicle (HF) is not only a skin accessory organ originating from the ectoderm but also a highly conserved sensory organ related to the pathogen-resistant immune response, thermoregulation, lipogenesis, angiogenesis, neurogenesis, wound healing, and social interactions [1, 2]. Therefore, the morphogenesis and regeneration of HF are especially important. The morphogenesis of HF is divided into three stages: induction, organogenesis, and cytodifferentiation during the embryo development process [3–5]. After birth, HF undergoes the circulatory process of damage and regeneration, namely, HF cycle, including anagen, catagen, and telogen [6, 7]. The interactions between epidermal and dermal mesenchymal cells determine the morphogenesis, development, and regeneration of HF, in which dermal papilla (DP) cells play a central regulatory role in signaling and regulating the homeostasis of neighboring cell populations [8–10]. Thus, DP cells are currently used to explore the molecular mechanism of HF development and regeneration.

Transcription factors play an essential role in HF development and regeneration by regulating gene expression [11–14], which control chromatin and transcription by recognizing specific DNA sequences to form complex systems that direct genome expression and regulate the processes of specifying cell types and developmental patterns [15]. Transcription factor CTIP2 promoted the expressions of *Lhx2* and *Nfatc1* genes by targeting their proximal promoter regions, thereby maintained HF stem cell pool during HF cycling [16]. Foxc1 activated *Nfatc1* and BMP signaling to reinforce quiescence in self-renewing HF stem cells [17]. Twist1 induced agglutinative growth and proliferation of DP cells by up-regulating the expression of *TCF4* [18]. Our previous study found hair cycle-specifically expressed transcription factors, such as HOXC13, SOX21, JUNB, and GATA3, indicating their important roles in HF differentiation stage [19]. Thus, it is of great significance to reveal their functions during HF development.

JUNB is a member of the dimer transcription factor AP-1 (activator protein-1) family, but its physiological function cannot be compensated by other AP-1 members, the most representative of which is the suppression of tumor cells proliferation [20–22]. However, whether JUNB regulates HF cell development is rarely studied. Therefore, this study aims to investigate the regulatory mechanism of JUNB during HF development, which would help illustrate the regulatory mechanism of hair development and regeneration, and provide new potential targets for molecular breeding of cashmere goats.

Materials and methods

Tissues collection and cell culture

Six pregnant Shanbei White cashmere goats (two years old, weighing 30–40 kg) were selected to obtain fetal skin samples at E65 (induction) and E120 (cytodifferentiation) [19]. And six female Shanbei White cashmere goats (one year old, coefficient of relationship < 0.125) were selected to obtain skin samples at anagen (during October) and telogen (during March of the following year). Each time point had three replicates. The specific steps of skin sample acquisition had been described in our previous article [23]. HEK293T and HEK293A cells (kept in our lab) were cultured in high-glucose DMEM (Hyclone, USA) supplemented with 1% double antibiotics (Penicillin and Streptomycin) and 10% FBS (Hyclone, USA) at 37 °C with 5% CO_2. DP cells were isolated from the secondary HFs of cashmere goats and cultured in DMEM/F12 media as previous described [23]. All the experimental procedures used in this study had been approved by the

Experimental Animal Manage Committee of Northwest A&F University.

Heatmap analysis and evolutionary tree mapping

The FPKM values of AP-1 family genes were screened out from the previous RNA-Seq results of skin samples (E65, E120, anagen, and telogen) [19, 24]. The data were sorted in csv format according to the corresponding period and transformed into R. Heatmaps were made by the R package. The specific FPKM values of each gene in each period are shown in Additional file 1: Tables S1 and S2. FASTA sequences of JUNB proteins of different species were obtained through NCBI database; then sequence comparison and evolutionary tree mapping were performed by MEGA software. The information of JUNB protein sequences from 11 different species is shown in Additional file 1: Table S3.

Real-time quantitative PCR (RT-qPCR)

The process of total RNA extraction and protocol of RT-qPCR were described as the previous study [23]. Gene-specific primers for amplification were designed using Primer Premier 6. RT-qPCR procedure was as follows: 95 °C for 3 min, following 40 cycles of 95 °C for 30 s and appropriate annealing temperatures for 30 s. The primers are listed in Table 1 and Additional file 1: Table S4.

Immunofluorescence staining

Skin tissues (from E65, E120, anagen, and telogen) were fixed with 4% paraformaldehyde and then prepared into paraffin sections [25]. The skin slides were processed by dewaxing, hydration, antigen retrieval, blocking, and antibody incubation, and experimental procedures were as described in previous study [26]. Cell immunofluorescence staining was fixed with 4% formaldehyde, followed by permeabilization, blocking, and antibody incubation as described as previous [27]. The results were observed under a fluorescence microscope. Hoechst 33342 (Beyotime Biotechnology, C1022) was used as nuclear staining reagent. Antibody-specific information is shown in Table 2.

Adenovirus and vector construction

The full-length ORF of *JUNB* was amplified by PCR using the cDNA from goat skin as a template. The amplified product was digested by *Not* I and *Xho* I and cloned into pAd-track-CMV vector. Then the vector was linearized with *Pme* I and cloned into pAd-Easy vector. The recombinant adenoviral vector was digested with *Pac* I and transfected into HEK293A cells for adenovirus packaging. The control group was the same as above.

The amplified products of *JUNB* CDS were digested by *Xba* I and *BamH* I and cloned into the pcDNA3.1 vector to construct the overexpression plasmid. The different length promoter regions of *TCF3* were amplified by PCR using goat genomic DNA as template. The amplified products were digested by *Not* I and *Kpn* I and cloned into the pGL3-basic vector. The predicted binding sites in *TCF3* promoter were mutated by introducing *EcoR* I (Mut-1) and *BamH* I (Mut-2) restriction sites. The primers are listed in Table 3.

Table 1 Real-time quantitative PCR primer information

Gene name	Accession no (Gene bank)	Primer sequence (5′-3′)	Product size (bp)	Tm (°C)
JUNB	XM_005682285.3	F: CAAGGGACACGCCTTCTGAG	166	60
		R: CAGGAGTCCAGTGTGGTTTG		
PCNA	XM_005688167.3	F: AAGAGGAGGAAGCTGTTACC	198	60
		R: CGATCTTGGGAGCCAAATAG		
MKi67	XM_005698601.3	F: GGACATTCAGACCCTAAGTG	180	60
		R: GTCTCGACGACTTCTGGTTC		
TCF3	XM_018050411.1	F: CCGTGTCGGTCATCCTGAAC	112	60
		R: TCTCCAACCACGCCTGATAC		
CTNNB1	XM_018066894.1	F:GAGGACAAGCCACAGGATTAT	101	58
		R: CCAAGATCAGCGGTCTCATT		
Cyclin D1	XM_018043271.1	F: GCAGTCTTAGGCATCCTGTAT	131	58
		R: CCTAGCCGAGAGGTTACATTA		
C-myc	XM_018058563.1	F: CAGAGGAGAAACGAGCTGAAA	130	62
		R: CTTGGACCGACAGGATGTATG		
β-actin	NM_001314342.1	F: TGAACCCCAAAGCCAACC	107	58
		R: AGAGGCGTACAGGGACAGCA		

Table 2 Antibodies information for immunofluorescence and western blot

Gene name	Name of antibody	Manufacturer	Size	Cat No.
JUNB	JUNB Polyclonal antibody	Proteintech	42 kDa	10486-1-AP
PCNA	PCNA Polyclonal antibody	Proteintech	–	10205-2-AP
Ki67	Anti-Ki67 rabbit polyclonal antibody	Sangon Biotech	–	D160529
TCF3	TCF3 Monoclonal antibody	Proteintech	–	67140-1-Ig
CTNNB1	Beta Catenin Polyclonal antibody	Proteintech	92 kDa	51067-2-AP
Cyclin D1	Cyclin D1 Polyclonal antibody	Proteintech	–	26939-1-AP
Cyclin D1	Cyclin D1 Monoclonal antibody	Proteintech	34 kDa	60186-1-Ig
C-myc	Purified Mouse Anti-Human C-Myc	BD Biosciences	62 kDa	551101
β-actin	Beta Actin Polyclonal antibody	Proteintech	42 kDa	20536-1-AP
–	HRP-conjugated Goat Anti-rabbit IgG	Sangon Biotech	–	D110058
–	HRP-conjugated Goat Anti-mouse IgG	Sangon Biotech	–	D110087
–	Donkey Anti-Rabbit IgG H&L	Abcam	–	ab150074

Table 3 Primer information for vector construction

Primer names	Sequence information (5′-3′)	Product size (bp)
JUNB CDS-pAd track-F	***ATTTGCGGCCGC***GACACCCGATACAGGCACAG	1154
JUNB CDS-pAd track-R	***CCCTCGAG***GGCTCAGAAGGCGTGTCCCTTG	
JUNB CDS-F	***CGGGATCC***CGGACACCCGATACAGGCACAG	1155
JUNB CDS-R	***GCTCTAGA***GCCTCAGAAGGCGTGTCCCTTG	
TCF3 promoter 717-F	***ATTTGCGGCCGC***TCTGTAGCGTCTACGATTCC	717
TCF3 promoter 717-R	***GGGGTACC***CCGAGAGCTGGGAGGATACTTG	
TCF3 promoter 1029-F	***ATTTGCGGCCGC***GCTTTCAGTCCTGCTCCTTG	1029
TCF3 promoter 1029-R	***GGGGTACC***CCGAGAGCTGGGAGGATACTTG	
TCF3 promoter 1284-F	***ATTTGCGGCCGC***CAAAGTGGCAAGAGCTTGAG	1284
TCF3 promoter 1284-R	***GGGGTACC***CCGAGAGCTGGGAGGATACTTG	
TCF3-717 mut 1-F	***CGGAATTC***CGGAAAGCTTTGAGAG	–
TCF3-717 mut 1-R	***CGGAATTC***CGTGAGTTCACTGAGA	–
TCF3-717 mut 2-F	***CGGGATCC***TATACGACTCTGC	–
TCF3-717 mut 2-R	***CGGGATCC***AGCCACTGAACT	–

The cleavage sites and their protective bases are shown in bolditalic

Western blot

DP cells were transfected with pAd-JUNB and pAd-NC; then the total protein was extracted using RIPA cell lysis solution after 48 h. The collected protein samples were transmembrane, sealed, and antibody incubated. The protocol of Western blot was described in our previous study [28]. β-Actin was used as the control. The gray value analysis of gel images was performed using Image J. Antibody information is shown in Table 2.

Functional analysis of DP cells

DP cells were seeded in 96-well plates at 1×10^4 cells per well and cultured for 48 h after pAd-JUNB and pAd-NC treatments; then the cell viability and proliferation of DP cells were assessed by MTT, CCK-8, EdU, and flow cytometry assays. For MTT analysis, the experimental procedure was described in our previous study [28]. The absorbance was measured at 490 nm using a Synergy H1 multidetector microplate reader (BioTek, Winooski, VT, USA). For CCK-8 assay analysis, 10 μL CCK-8 solution were added to each well and incubated for 4 h at 37 °C, 5% CO_2. Absorbance was measured at 450 nm. EdU assay was performed according to Cell-Light EdU DNA cell proliferation kit (RiboBio, C10310-1/-2/-3, China), and EdU-positive cells were observed under a fluorescence microscope. For flow cytometry assay, DP cells were seeded in 60 mm dishes and the specific experimental procedure was described in a previous study [27]. The data were analyzed using CytExpert system.

Dual-luciferase activity assay

The binding sites between JUNB and *TCF3* were predicted through JASPAR (https://jaspar.genereg.net/), and the dual-luciferase vectors were constructed. The possible interactions between JUNB and *TCF3* were identified by dual-luciferase assay in HEK293T cells, which were seeded in a 24-well plate, and plasmids were transfected with Lipofectamine6000 (Beyotime Biotechnology, C0526) when the cell density reached 80%. Then, the luciferase activity was measured by dual-luciferase reporter kit (Promega). Each experiment was repeated at least three times. The *TCF3* 717 bp promoter fragment without JUNB binding sites mutation was named Wt, with mutation of one binding site was named Mut-1 or Mut-2, and with mutation of both binding sites was named Mut-1 + 2.

In vivo injection of adenovirus

C57 BL/6 strain mice were purchased from Chengdu Dossy Experimental Animals Co., Ltd and were housed in a temperature-controlled room with ad libitum food and water. The skin samples were collected after experimental treatment. Every skin sample was divided into two parts: one was fixed with 4% paraformaldehyde and the other was frozen in sample protector for RNA extraction (Takara, China) and stored at − 80 °C for subsequent analyses.

Male C57 BL/6 mice at postnatal day 56 were anesthetized with 1% pentobarbital sodium and shaved back hairs. A mixture of 50 μL of adenovirus and 200 μL of normal saline was injected subcutaneously along the midline of the back skin. The skin and HF of mice were observed every day. Mice were sacrificed to perform skin tissue sections and H&E staining analysis at 10 d, 25 d, and 35 d post-injection. The specific procedures of skin tissue sections and H&E staining were described in previous study [25]. KI67 immunofluorescence staining was performed on mouse skin tissue sections at 10 d and 25 d post-injection to observe the expression of KI67 in HFs, especially in DP region.

Statistical analysis

The fold change of mRNA expression was analyzed using the $2^{-\triangle\triangle CT}$ method. *β-actin* was used as internal control to normalize the data. The data were analyzed using GraphPad Prism 7.0 software (GraphPad Software, San Diego, CA, USA) with *t*-test. Data are presented as mean ± standard error (SEM), and statistical significance was considered as $^{*}P < 0.05$, $^{**}P < 0.01$, and $^{***}P < 0.001$.

Results

Expression of JUNB in HF at different periods

Based on our previous transcriptome sequencing data of skin tissues from Shanbei White cashmere goats (induction, cytodifferentiation, anagen, and telogen) [19, 24], it was found that 25 genes of the AP-1 family showed a trend of differential expression among these periods (Fig. 1A). RT-qPCR result further showed that the expression of *JUNB* in induction (E 65) was significantly lower than that in cytodifferentiation (E 120) at embryo stage, and its expression in telogen was significantly higher than that in anagen, which were consistent with the sequencing result (Fig. 1B). The immunofluorescence staining further indicated that JUNB expressed in dermal papilla region (Fig. 1C); therefore, the following function study of JUNB was explored in DP cells.

JUNB promoted the proliferation of DP cells

The adenovirus overexpression system was used to determine the effect of JUNB on DP cells. RT-qPCR and Western blot results showed that the expression of JUNB was significantly increased after pAd-JUNB transfection for 48 h. The immunofluorescence staining assay was consistent with the results of RT-qPCR and Western blot (Additional file 1: Fig. S1). Cell cycle analysis indicated that the percentage of DP cells in S phase and G2 phase were higher than those in the control group (Fig. 2A). With the overexpression of JUNB, the proliferation of DP cells was significantly increased compared with the control by using EdU assay (Fig. 2B). MTT and CCK-8 analysis further showed that the cell viability was significantly increased compared with the control group (Fig. 2C and D). In addition, the expressions of cell proliferation-related marker genes, such as *PCNA* and *MKi67*, were significantly higher with the overexpression of JUNB compared with the control group by RT-qPCR and immunofluorescence staining (Fig. 2E and F). The aforementioned results indicated that JUNB promoted the proliferation of DP cells.

JUNB regulated *TCF3* by targeting its promoter

The target genes of JUNB were predicted by using bioinformatics software, 41 genes were obtained, and the specific information is shown in Additional file 1: Table S5. Go and KEGG analysis demonstrated that the target genes of JUNB were significantly enriched in Wnt signaling pathway, including *GSK3β*, *SMAD4*, *CREBBP*, *TCF3*, *JUN*, and *EP300* genes (Additional file 1: Fig. S2). LEF/TCF family is the most important transcription factor mediating Wnt/β-catenin signaling, and the DNA-binding motif of JUNB was on the promoter of *TCF3* through JASPAR database.

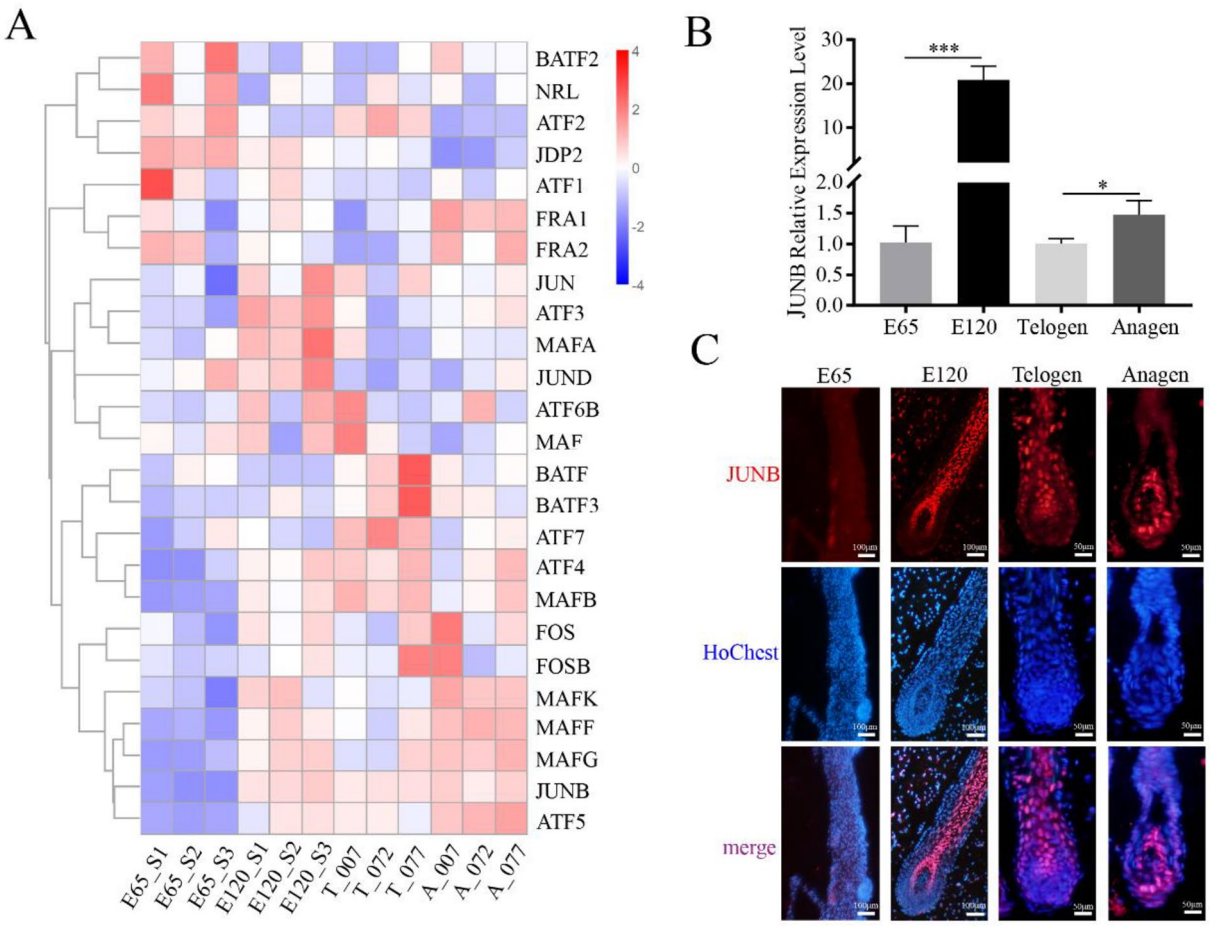

Fig. 1 JUNB screening and differential expression validation. **A** Heatmap analysis of the expression of AP-1 family genes. E65 is induction stage, E120 is cytodifferentiation stage, A is anagen stage, and T is telogen stage. **B** Relative mRNA expression of *JUNB* at E65, E120, telogen, and anagen. **C** Immunofluorescence staining of JUNB in cashmere goat HFs at E65, E120, telogen, and anagen. The data are expressed as the mean ± SE ($n = 3$). ***$P < 0.001$, *$P < 0.05$. Scale bars, 50 μm, 100 μm

Therefore, *TCF3* gene was screened as the target gene of JUNB (Fig. 3A and B). The optimal promoter of *TCF3* gene was detected by pGL3-basic system, and the result showed that the 717 bp fragment at the promoter was the core region of *TCF3* (Fig. 3C); then the dual-luciferase assay and binding site mutation assay were further performed to validate it. The luciferase activity of the promoter without mutation was significantly higher than the control group after *JUNB* overexpressed, indicating that JUNB could promote the transcription of *TCF3* gene. The luciferase activity of the promotor with one mutation (Mut-1 or Mut-2) was still significantly higher than the control, while the luciferase activity with two mutations at the promoter had no significant difference compared with the control group, revealing that *JUNB* regulated the transcription of *TCF3* by binding to these two sites (Fig. 3D). Furthermore, the expression of *TCF3* was significantly increased after *JUNB* overexpressed in DP cells by RT-qPCR and immunofluorescence staining methods (Fig. 3E and F), revealing that JUNB targeted the promoter region of *TCF3* to regulate its expression.

JUNB activated Wnt signaling pathway in DP cells

To explore the potential regulatory mechanism of JUNB, we further detected the expression of Wnt signaling pathway-related genes. β-catenin is a central regulatory factor in Wnt signaling pathway and competitively binds to the LEF/TCF transcription factors to activate their downstream genes [29, 30]. Immunofluorescence staining and Western blot results showed that the expression of β-catenin was increased after *JUNB* overexpressed in DP cells. And the expression trends of Cyclin D1 and C-myc, the downstream cell proliferation factors, were also consistent with β-catenin (Fig. 4A and B). RT-qPCR

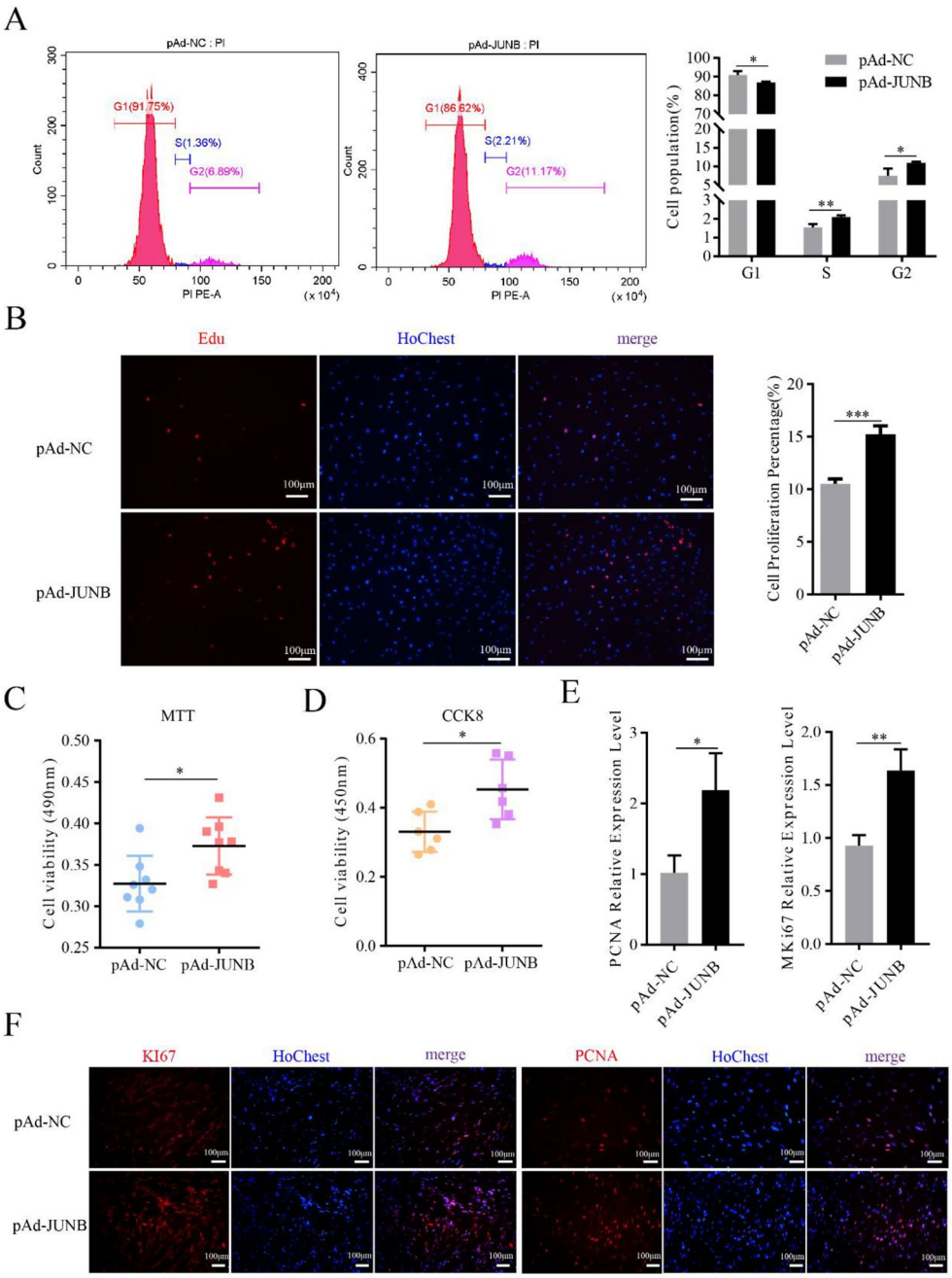

Fig. 2 Effect of JUNB on DP cells viability, proliferation, and cell cycle. **A** Flow cytometry analysis of DP cells cycle after pAd-JUNB and pAd-NC infection for 48 h. Statistical analysis of the proportion of cells in each cell cycle. **B** EdU staining analysis of DP cells proliferation following 48 h of pAd-JUNB and pAd-NC infection treatments. Statistical analysis of the number of EdU-positive cells. **C** MTT analysis of DP cells viability after pAd-JUNB and pAd-NC infection for 48 h. **D** CCK-8 analysis of DP cells viability after pAd-JUNB and pAd-NC infection for 48 h. **E** RT-qPCR result of cell proliferation marker gene *PCNA* and *MKi67* after pAd-JUNB and pAd-NC infection for 48 h. **F** Immunofluorescence staining of PCNA and Ki67 after pAd-JUNB and pAd-NC infection for 48 h. The data are expressed as the mean ± SE ($n = 3$). *$P < 0.05$, **$P < 0.01$, ***$P < 0.001$. Scale bars, 100 μm

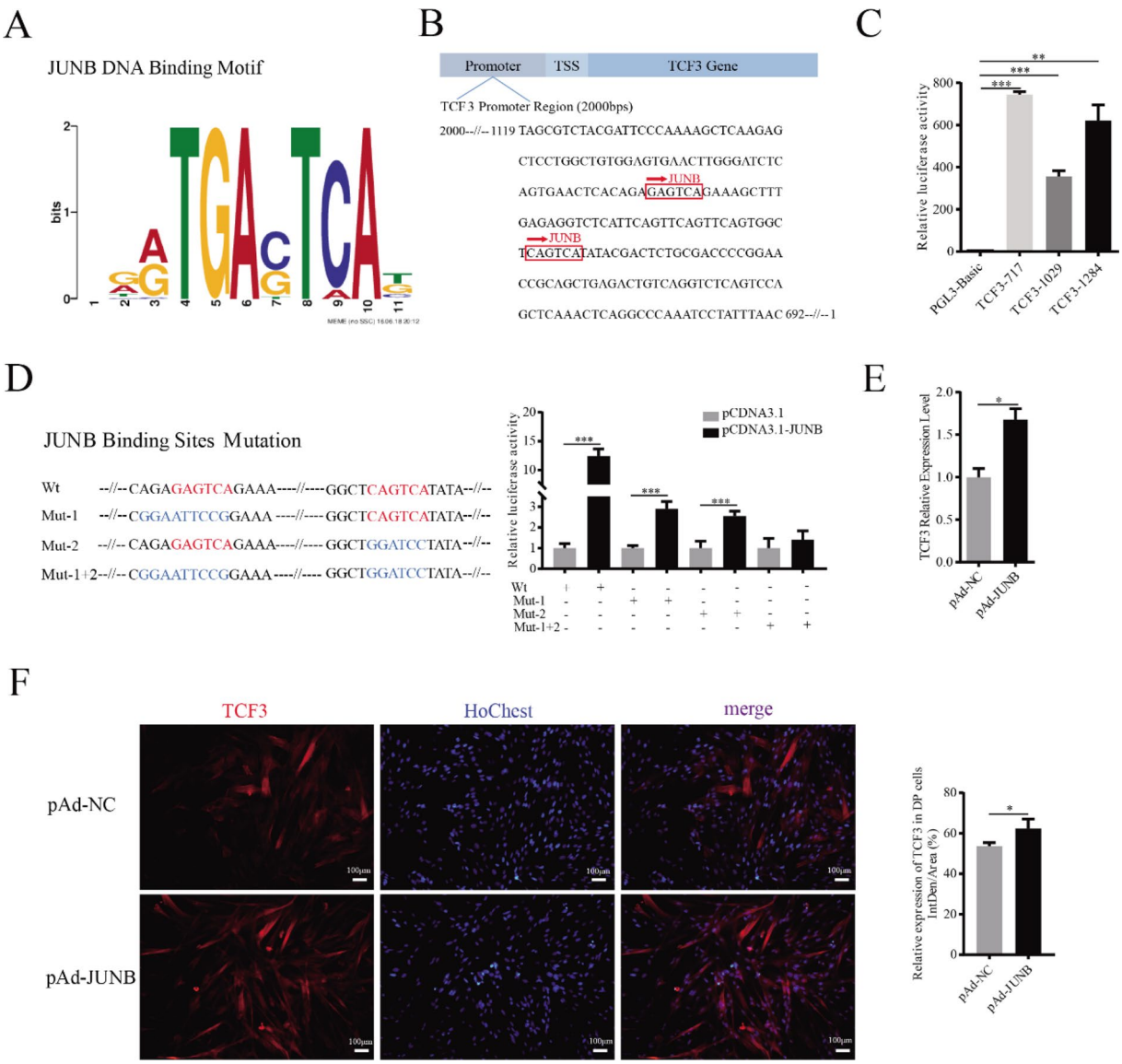

Fig. 3 The mechanism verification of *JUNB* regulating *TCF3*. **A** The DNA-binding motif of JUNB from JASPAR database. **B** The transcription binding sites of *JUNB* on the *TCF3* promoter region. **C** Dual-luciferase assay to detect the optimal promoter activity of *TCF3* in HEK293T cells. **D** The mutation of *JUNB* transcriptional binding sites on the *TCF3* promoter region, and dual-luciferase assay to detect the interaction between *JUNB* and *TCF3* in HEK293T cells. Binding sites are marked in red and mutated binding sites are marked in blue. **E** RT-qPCR analysis of *TCF3* expression after pAd-JUNB and pAd-NC infection for 48 h in DP cells. **F** Immunofluorescence staining of TCF3 after pAd-JUNB and pAd-NC infection for 48 h in DP cells. The mean fluorescence intensity was analyzed by Image J. IntDen is the total fluorescence intensity of the region, and area is the extent of the region. The data are expressed as the mean ± SE ($n = 3$). *$P < 0.05$, **$P < 0.01$, ***$P < 0.001$. Scale bars, 100 μm

result further supported these findings (Fig. 4C). These results revealed that JUNB promoted DP cell proliferation by activating Wnt signaling pathway.

JUNB promoted the development and regeneration of mouse hair in vivo

The in vivo experiment was further explored to verify the function and regulation mechanism of JUNB in HF development and regeneration. The homology of JUNB protein sequence among different species showed that there was high homology between goat and mouse (Fig. 5); therefore, C57 BL/6 mice was taken as the model. The pAd-JUNB and pAd-NC were subcutaneously injected into the skin of C57 BL/6 mice (Fig. 6A). The expression of *JUNB* in the back skin was significantly increased with the injection with pAd-JUNB than the control group by RT-qPCR analysis (Additional file 1: Fig. S3A). The back hair injected with pAd-JUNB grew

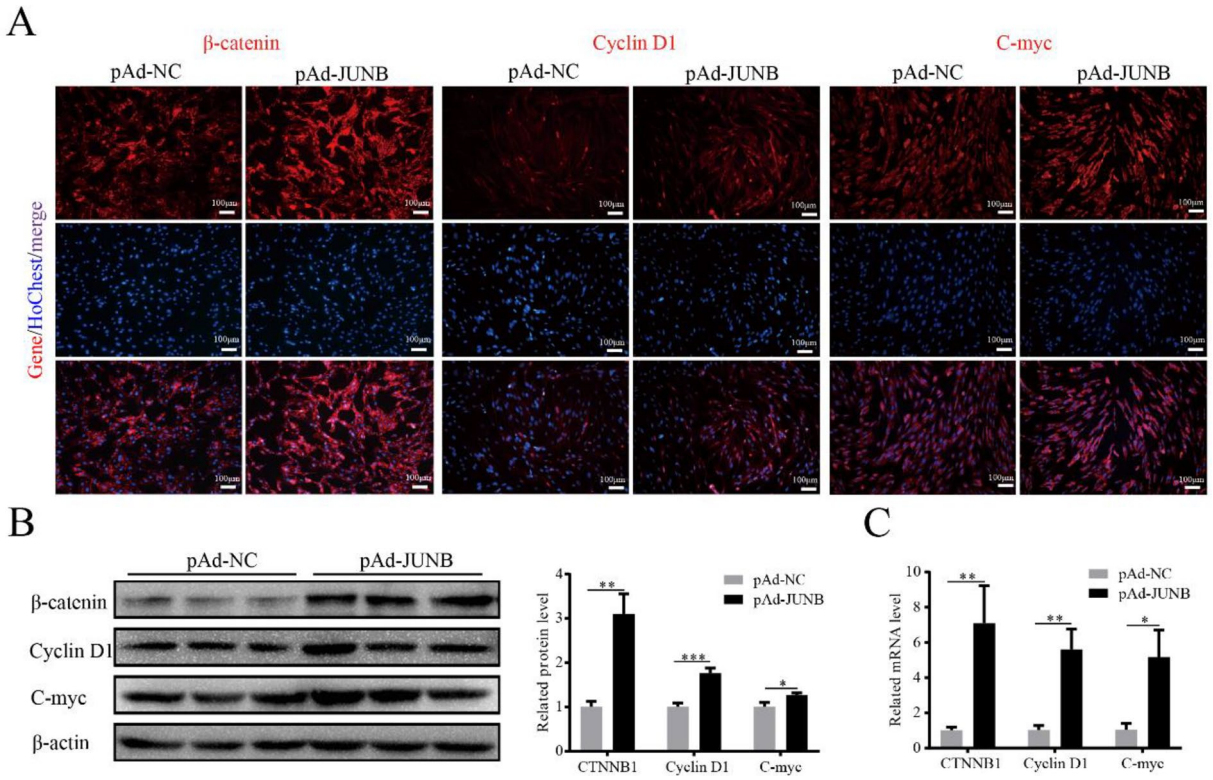

Fig. 4 JUNB promoted the expression of Wnt/β-catenin signaling pathway genes in DP cells. **A** Immunofluorescence staining of β-catenin, Cyclin D1, and C-myc after pAd-JUNB and pAd-NC infection for 48 h in DP cells. **B** Western blot analysis of β-catenin, Cyclin D1, and C-myc after pAd-JUNB and pAd-NC infection for 48 h in DP cells. The grayscale of Western blot was analyzed by Image J. **C** RT-qPCR result of *CTNNB1*, *Cyclin D1*, and *C-myc* after pAd-JUNB and pAd-NC infection for 48 h in DP cells. The data are expressed as the mean ± SE ($n = 3$). *$P < 0.05$, **$P < 0.01$, ***$P < 0.001$. Scale bars, 100 μm

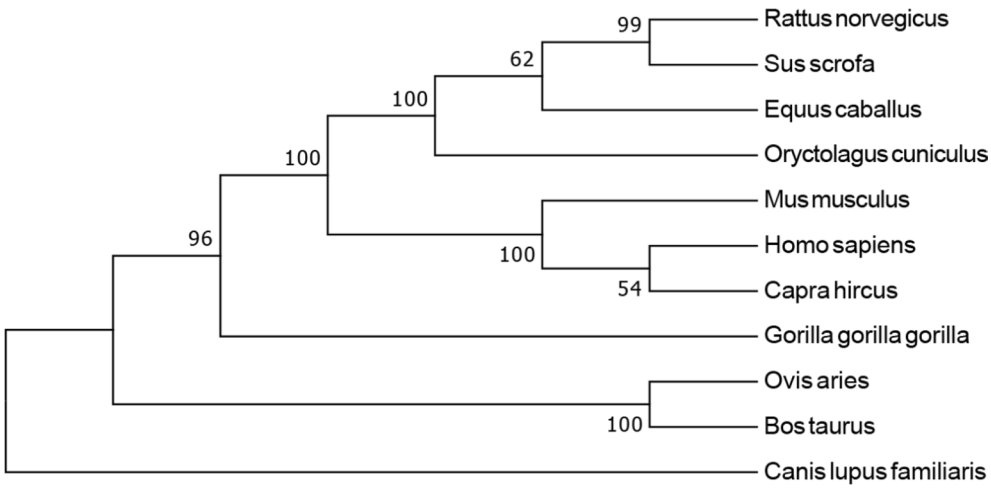

Fig. 5 Homology analysis of JUNB protein sequences among different species. The protein sequence information was obtained from the NCBI database for a total of 11 species. The information of 11 species was as follows: cattle (*Bos taurus*), dog (*Canis lupus familiaris*), goat (*Capra hircus*), horse (*Equus caballus*), house mouse (*Mus musculus*), human (*Homo sapiens*), Norway rat (*Rattus norvegicus*), pig (*Sus scrofa*), rabbit (*Oryctolagus cuniculus*), sheep (*Ovis aries*), and western lowland gorilla (*Gorilla gorilla gorilla*)

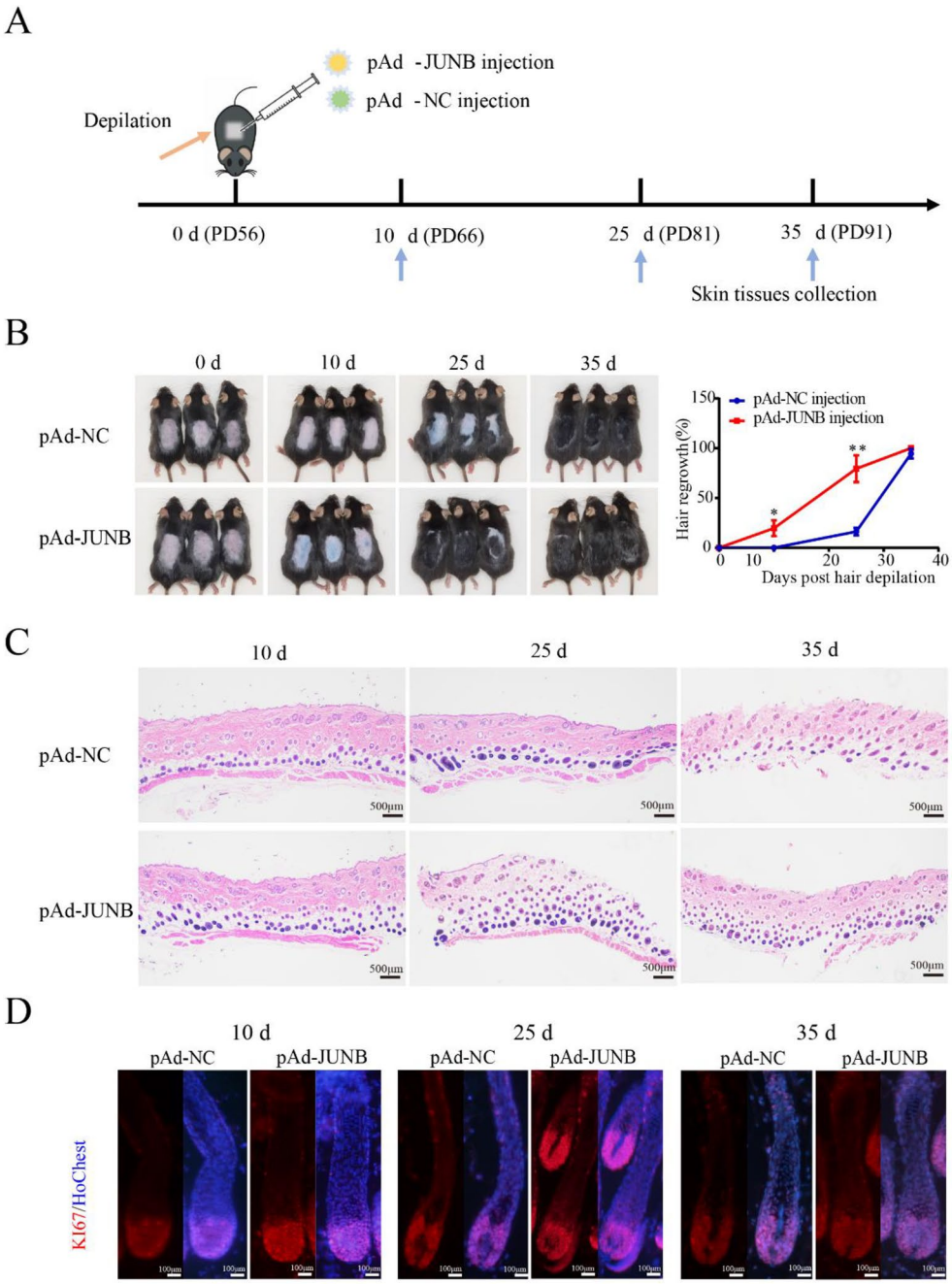

Fig. 6 JUNB promoted the hair regeneration of mouse back skin. **A** Schematic diagram of mouse back skin treatment. **B** Hair growth of mouse back skin after injection of pAd-JUNB and pAd-NC at 0 d, 10 d, 25 d, and 35 d, respectively. Statistical analysis of hair regeneration on the mouse back skin injected with pAd-JUNB and pAd-NC at 0 d, 10 d, 25 d, and 35 d, respectively. **C** HE staining analysis of the mouse back skin injected with pAd-JUNB and pAd-NC at 10 d, 25 d, and 35 d, respectively. **D** Immunofluorescence staining of Ki67 on the mouse back skin injected with pAd-JUNB and pAd-NC at 10 d, 25 d, and 35 d, respectively. The data are expressed as the mean ± SE ($n = 3$). *$P < 0.05$, **$P < 0.01$. Scale bars, 100 μm, 500 μm

significantly faster than the control group. After 10 d of the treatment, the two groups showed significant difference at back hair areas, and the difference enlarged after 25 d, then basically all overgrown at 35 d (Fig. 6B). The number of regenerated HFs injected with pAd-JUNB was significantly more than that of the control group by HE staining (Fig. 6C). Meanwhile, the expressions of Wnt signaling pathway-related genes were significantly higher in the pAd-JUNB injection group than the control, which was consistent with the results at cellular level

(Additional file 1: Fig. S3B–E). In addition, immunofluorescence staining showed that the expression of Ki67 was higher in the HFs injected with pAd-JUNB, and significantly higher in DP cells at 10 d and 25 d, but there was no significant difference at 35 d (Fig. 6D). Taken together, this study demonstrated that JUNB enhanced Wnt signaling pathway activity by targeting *TCF3* gene expression, thereby promoting the proliferation of DP cells and affecting hair regeneration.

Discussion

HF is the main unit that produces a single visible hair shaft, and its number and characteristics affect hair growth and regeneration. HFs have complex structures and diverse cell types, and their development involves signal exchanges between different types of cells, especially the interaction between surface epithelial cells and dermal cells [31–33]. The regeneration of HFs also depends on the active communication between epidermal stem cells and dermal papilla cells, also known as epithelial–mesenchymal interaction (EMI) [34, 35]. During these processes, many functional genes are regulated at transcriptional, post-transcriptional, and epigenetic levels, thus showing activating or silencing state. Transcription factors play a decisive role in gene transcription during HF development and regeneration [14, 36]. Foxi3 displays a highly dynamic expression pattern during hair morphogenesis and cycling, and the lack of Foxi3 reduces the specification and activation of HF stem cell, and poor hair regeneration upon hair plucking [37]. Loss of Hes1 results in delayed activation of secondary hair germ (HG) and shortened anagen phase, and Hes1 could potentiate Shh signaling in anagen initiation to maintain hair cycle homeostasis [38]. In addition, other transcription factors also play important roles during the development of HFs, such as LHX2, JUNB, RUNX1, and VDR [19, 39].

JUNB is an important subunit of the transcriptional activator protein AP-1 (activator protein-1), involving in the regulation of various cellular physiological functions [21, 40]. AP-1 family members have a highly conserved basic leucine zipper domain bZip, in which the leucine zipper domain LZ is mainly a dimer-forming region, and the basic region BR is used to bind DNA sequences [41, 42]. JUNB plays an antagonistic role (transcriptional repressor or activator) in cell cycle regulation, but the manifestations of these two opposing properties depend on the stage of cell cycle and environmental conditions [20, 43–45]. The glucocorticoid receptor GR interacts with the transcription factor JUNB in multiple cell types, including keratinocytes, to down-regulate its expression and significantly alter HF development [46]. After the induction of JUNB deletion in mice, the proliferation of HF stem cells in the carina was promoted, which in turn triggered the phenomenon of epidermal hyperplasia [47]. LncRNA MSTRG14109.1 and circRNA452 competed with miRNA-2330 to regulate the expression of *TCHH*, *KRT35,* and *JUNB*, thereby further regulated cashmere fineness [48]. These results revealed the important roles of JUNB in HF development and regeneration through regulating HF cells.

Our previous studies have found that JUNB is highly expressed in HF cytodifferentiation and anagen stages, indicating its role in HF development and cycling [19, 24]. However, there are no evidence revealing that JUNB regulates HF development and regeneration, and the effect on HF dermal derived cells is unclear, which still needs to be further studied. In this study, we demonstrated that the expression levels of JUNB in cytodifferentiation and anagen were significantly higher than those in induction and telogen, and JUNB was expressed at the dermal papilla. Therefore, we hypothesized that JUNB may affect the physiological function of DP cells. This study found that JUNB could promote HF development and regeneration by promoting the proliferation of DP cells.

However, the downstream regulatory mechanism of JUNB is not well elucidated. Based on bioinformatics analysis, we found the potential binding sites of JUNB at the promoter of *TCF3* and hypothesized that JUNB could influence the activity of *TCF3* promoter, thereby regulating Wnt/β-catenin signaling pathway and leading to the proliferation of DP cells. Wnt/β-catenin signaling pathway involves in the developmental processes and fate selection during tissue morphogenesis by regulating cell proliferation, migration, and differentiation [49–51]. β-catenin cooperates with the members of TCF/LEF family of transcription factors (TCF1, TCF3, TCF4, LEF1) to regulate gene expression [52, 53]. Previous studies have shown that the stable expression of β-catenin in HF stem cells at the bulge activates the LEF/TCF complex and the transcription of downstream target genes, thereby promoting the activation, proliferation, and directed differentiation of HF stem cells [54]. The loss of Sfrp1 (a Wnt antagonist) showed a depletion of HFSCs, enhanced HFSC proliferation, and accelerated HF cycle at PD21-PD28 [55]. Our data suggested that JUNB elevated the expression of *TCF3* and regulated the Wnt/β-catenin signaling pathway, as well as the downstream gene expression including *c-Myc* and *Cyclin D1* genes. Further mechanism studies demonstrated that JUNB could directly bind to the promoter region of *TCF3* and enhance the promoter activity and the final expression of *TCF3*.

DP cells play important roles in HF development, and the aforementioned results revealed that JUNB promoted the proliferation of DP cells at the cellular level, and the

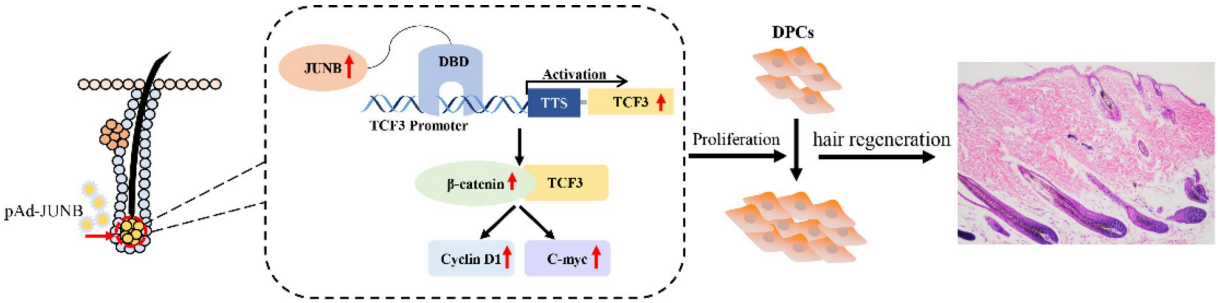

Fig. 7 Model summarizing the main findings of this study. DBD is a DNA-binding domain that recognizes a specific DNA sequence

evidence was relatively insufficient. Due to the high feeding cost, long HF cycle and difficult phenotype observation of goat species, it is not feasible to conduct in vivo experiments on goats. Therefore, we conducted comparison and homology analysis of JUNB protein sequences from different species in order to determine a suitable animal model. The results showed that the protein sequence of JUNB had high homology in goat and mouse, and C57 BL/6 mice were selected as the animal model for in vivo experiment. Subsequently, we performed in vivo experiment to further verify the function of JUNB on HF development and regeneration. The result demonstrated that JUNB could promote hair development and regeneration. Moreover, we also found that JUNB could significantly increase the number of regenerated HFs, improve the protein expression of KI67 in DP, and elevate the mRNA expression of Wnt/β-catenin signaling pathway-related genes. These results were consistent with the in vitro results at molecular level, which further confirmed that JUNB could promote the proliferation of DP cells and enhance the activity of Wnt/β-catenin signaling pathway. In order to further improve the results of in vivo experiments, a conditional knockout of JUNB mouse model would be constructed to detect the hair phenotype data and make the evidence more comprehensive in the future. The in vivo experiment of cashmere goats takes a long time and costs a lot. However, there are still significant species differences between mice and cashmere goats, and the in vivo experiment results of mice cannot fully represent cashmere goats. Therefore, the subsequent in vivo experiments should be conducted on cashmere goats as much as possible under allowable conditions.

Conclusions

In summary, our findings imply that JUNB plays a vital role in hair growth and regeneration process. We found that JUNB downstream target genes are mainly enriched in the process of RNA polymerase II core promoter proximal region sequence-specific DNA binding through using bioinformatics analysis. And JUNB directly regulates the expression of *TCF3* by binding to its core promoter region, enhances the activity of Wnt/β-catenin signaling pathway, and promotes the proliferation of DP cells (Fig. 7). Thus, JUNB might be a useful target for improving cashmere quality and breeding of cashmere goats.

Supplementary Information

The online version contains supplementary material available at https://doi.org/10.1186/s40538-023-00499-0.

Additional file 1: Fig S1. The overexpression of JUNB in DP cells. **A** RT-qPCR analysis of *JUNB* after infection with pAd-JUNB and pAd-NC for 48 h. **B** western blot analysis of JUNB after infection with pAd-JUNB and pAd-NC for 48 h. The grayscale of western blot was analyzed by Image J. **C** immunofluorescence staining of JUNB after infection with pAd-JUNB and pAd-NC for 48 h. The data was expressed as the mean ± SE ($n = 3$). $^{**}P < 0.01$, $^{***}P < 0.001$. Scale bars, 100 μm. **Fig S2.** Prediction and bioinformatics analysis of *JUNB* target genes. **A** The target genes of JUNB were predicted using Harmonizome, Cistrome DB and hTFtarget databases. **B** KEGG pathway analysis of JUNB target genes. **C** GO analysis of JUNB target genes. **Fig S3.** The expression of *JUNB* and Wnt signaling pathway-related genes in mouse back skin after treatment. **A** RT-qPCR analysis of *JUNB* on the mouse back skin injected with pAd-JUNB and pAd-NC at 0 d, 10 d, 25 d, and 35 d respectively. **B** RT-qPCR analysis of *CTNNB1* on the mouse back skin injected with pAd-JUNB and pAd-NC at 0 d, 10 d, 25 d, and 35 d respectively. **C** RT-qPCR analysis of *TCF3* on the mouse back skin injected with pAd-JUNB and pAd-NC at 0 d, 10 d, 25 d, and 35 d respectively. **D** RT-qPCR analysis of *Cyclin D1* on the mouse back skin injected with pAd-JUNB and pAd-NC at 0 d, 10 d, 25 d, and 35 d respectively. **E** RT-qPCR analysis of *C-myc* on the mouse back skin injected with pAd-JUNB and pAd-NC at 0 d, 10 d, 25 d, and 35 d respectively. The data were expressed as the mean ± SE (n = 3). $^{*}P < 0.05$, $^{**}P < 0.01$, $^{***}P < 0.001$. **Table S1.** Sequencing results of AP-1 family genes in embryonic skin tissues of Shaanbei white Cashmere goats. **Table S2.** Sequencing results of AP-1 family genes in skin tissues of Shaanbei White Cashmere Goats at Anagen and Telogen Stages. **Table S3.** The information of JUNB protein sequences from 11 different species. **Table S4.** Real-time quantitative PCR primer information of mouse. **Table S5.** Statistics of JUNB target genes.

Acknowledgements

The authors are grateful to Yuelang Zhang (Hainan Institute, Zhejiang University) for helping with data analysis.

Author contributions

TZ and XW designed the research. TZ, FL, XL, XZ, and YZ performed the experiments and analyzed the data. TZ wrote the manuscript. XW has primary responsibility for writing—review and editing. All the authors have read and approved the published version of the manuscript.

Funding
This work was supported by the National Natural Science Foundation of China (No. 31972556).

Availability of data and materials
Data sharing is not applicable to this article as no datasets were generated or analyzed during the current study.

Declarations

Ethics approval and consent to participate
All the experimental procedures used in this study had been approved by the Experimental Animal Manage Committee of Northwest A&F University.

Consent for publication
Not applicable.

Competing interests
The authors declare that they have no competing interests.

Author details
[1]Key Laboratory of Animal Genetics, Breeding and Reproduction of Shaanxi Province, College of Animal Science and Technology, Northwest A&F University, Yangling 712100, Shaanxi, China.

Received: 19 September 2023 Accepted: 27 October 2023
Published online: 13 November 2023

References

1. Bernard BA. La biologie du follicule pileux [The biology of hair follicle]. J Soc Biol. 2005;199(4):343–8.
2. Park S. Hair follicle morphogenesis during embryogenesis, neogenesis, and organogenesis. Front Cell Dev Biol. 2022;10:933370.
3. Kumamoto T, Shalhevet D, Matsue H, Mummert ME, Ward BR, Jester JV, et al. Hair follicle serve as local reservoirs of skin mast cell precursors. Blood. 2003;102(5):1654–60.
4. Forni MF, Trombetta-Lima M, Sogayar MC. Stem cells in embryonic skin development. Biol Res. 2012;45(3):215–22.
5. Lin X, Zhu L, He J. Morphogenesis, growth cycle and molecular regulation of hair follicles. Front Cell Dev Biol. 2022;10:899095.
6. Botchkarev VA, Kishimoto J. Molecular control of epithelial-mesenchymal interactions during hair follicle cycling. J Investig Dermatol Symp Proc. 2003;8(1):46–55.
7. Houschyar KS, Borrelli MR, Tapking C, Popp D, Puladi B, Ooms M, et al. Molecular mechanisms of hair growth and regeneration: current understanding and novel paradigms. Dermatology. 2020;236(4):271–80.
8. Legué E, Nicolas JF. Hair follicle renewal: organization of stem cells in the matrix and the role of stereotyped lineages and behaviors. Development. 2005;132(18):4143–54.
9. Driskell RR, Clavel C, Rendl M, Watt FM. Hair follicle dermal papilla cells at a glance. J Cell Sci. 2011;124(Pt 8):1179–82.
10. Ji S, Zhu Z, Sun X, Fu X. Functional hair follicle regeneration: an updated review. Signal Transduct Target Ther. 2021;6(1):66.
11. Fernandez-Guerrero M, Yakushiji-Kaminatsui N, Lopez-Delisle L, Zdral S, Darbellay F, Perez-Gomez R, et al. Mammalian-specific ectodermal enhancers control the expression of *Hoxc* genes in developing nails and hair follicle. Proc Natl Acad Sci USA. 2020;117(48):30509–19.
12. Bhat B, Yaseen M, Singh A, Ahmad SM, Ganai NA. Identification of potential key genes and pathways associated with the Pashmina fiber initiation using RNA-Seq and integrated bioinformatics analysis. Sci Rep. 2021;11(1):1766.
13. Veltri A, Lang CMR, Cangiotti G, Chan CK, Lien WH. ROR2 regulates self-renewal and maintenance of hair follicle stem cells. Nat Commun. 2022;13(1):4449.
14. Yang Q, Zhang J, Bao Q, Zhong J, Wang X, Tao Y, et al. Foxp1 and Foxp4 deletion causes the loss of follicle stem cell niche and cyclic hair shedding by inducing inner bulge cell apoptosis. Stem Cells. 2022;40(9):843–56.
15. Lambert SA, Jolma A, Campitelli LF, Das PK, Yin Y, Albu M, et al. The human transcription factors. Cell. 2018;172(4):650–65.
16. Bhattacharya S, Wheeler H, Leid M, Ganguli-Indra G, Indra AK. Transcription factor CTIP2 maintains hair follicle stem cell pool and contributes to altered expression of LHX2 and NFATC1. J Invest Dermatol. 2015;135(11):2593–602.
17. Wang L, Siegenthaler JA, Dowell RD, Yi R. Foxc1 reinforces quiescence in self-renewing hair follicle stem cells. Science. 2016;351(6273):613–7.
18. Yu N, Hu T, Yang H, Zhang L, Song Q, Xiang F, et al. Twist1 contributes to the maintenance of some biological properties of dermal papilla cells *in vitro* by forming a complex with Tcf4 and β-catenin. Front Cell Dev Biol. 2020;8:824.
19. Wang S, Li F, Liu J, Zhang Y, Zheng Y, Ge W, et al. Integrative analysis of methylome and transcriptome reveals the regulatory mechanisms of hair follicle morphogenesis in cashmere goat. Cells. 2020;9(4):969.
20. Piechaczyk M, Farràs R. Regulation and function of JunB in cell proliferation. Biochem Soc Trans. 2008;36(Pt 5):864–7.
21. Gazon H, Barbeau B, Mesnard JM, Peloponese JM. Hijacking of the AP-1 signaling pathway during development of ATL. Front Microbiol. 2018;8:2686.
22. Katagiri T, Kameda H, Nakano H, Yamazaki S. Regulation of T cell differentiation by the AP-1 transcription factor JunB. Immunol Med. 2021;44(3):197–203.
23. Wang S, Luo Z, Zhang Y, Yuan D, Ge W, Wang X. The inconsistent regulation of HOXC13 on different keratins and the regulation mechanism on HOXC13 in cashmere goat (*Capra hircus*). BMC Genomics. 2018;19(1):630.
24. Wang S, Ge W, Luo Z, Guo Y, Jiao B, Qu L, et al. Integrated analysis of coding genes and non-coding RNAs during hair follicle cycle of cashmere goat (*Capra hircus*). BMC Genomics. 2017;18(1):767.
25. Ge W, Zhao Y, Lai FN, Liu JC, Sun YC, Wang JJ, et al. Cutaneous applied nano-ZnO reduce the ability of hair follicle stem cells to differentiate. Nanotoxicology. 2017;11(4):465–74.
26. Ge W, Tan SJ, Wang SH, Li L, Sun XF, Shen W, et al. Single-cell transcriptome profiling reveals dermal and epithelial cell fate decisions during embryonic hair follicle development. Theranostics. 2020;10(17):7581–98.
27. Zhang W, Wang N, Zhang T, Wang M, Ge W, Wang X. Roles of melatonin in goat hair follicle stem cell proliferation and pluripotency through regulating the Wnt signaling pathway. Front Cell Dev Biol. 2021;9:686805.
28. Zhang Y, Xia S, Wang T, Wang S, Yuan D, Li F, et al. Chi-miR-30b-5p inhibits dermal papilla cells proliferation by targeting CaMKIIδ gene in cashmere goat. BMC Genomics. 2020;21(1):430.
29. Veltri A, Lang C, Lien WH. Concise review: Wnt signaling pathways in skin development and epidermal stem cells. Stem Cells. 2018;36(1):22–35.
30. Koelman EMR, Yeste-Vázquez A, Grossmann TN. Targeting the interaction of β-catenin and TCF/LEF transcription factors to inhibit oncogenic Wnt signaling. Bioorg Med Chem. 2022;70:116920.
31. Nowak JA, Polak L, Pasolli HA, Fuchs E. Hair follicle stem cells are specified and function in early skin morphogenesis. Cell Stem Cell. 2008;3(1):33–43.
32. Dai B, Sha RN, Yuan JL, Liu DJ. Multiple potential roles of thymosin β4 in the growth and development of hair follicles. J Cell Mol Med. 2021;25(3):1350–8.
33. Zheng Q, Zhang X, Bao P, Zhou X, Chu M, Guo X, et al. Understanding mammalian hair follicle ecosystems by single-cell RNA sequencing. Animals. 2022;12(18):2409.
34. Chang KW, Huang NA, Liu IH, Wang YH, Wu P, Tseng YT, et al. Emergence of differentially regulated pathways associated with the development of regional specificity in chicken skin. BMC Genomics. 2015;16(1):22.
35. Ohyama M. Use of human intra-tissue stem/progenitor cells and induced pluripotent stem cells for hair follicle regeneration. Inflamm Regen. 2019;39:4.
36. Lee SE, Sada A, Zhang M, McDermitt DJ, Lu SY, Kemphues KJ, et al. High Runx1 levels promote a reversible, more-differentiated cell state in hair-follicle stem cells during quiescence. Cell Rep. 2014;6(3):499–513.
37. Shirokova V, Biggs LC, Jussila M, Ohyama T, Groves AK, Mikkola ML. Foxi3 deficiency compromises hair follicle stem cell specification and activation. Stem Cells. 2016;34(7):1896–908.
38. Suen WJ, Li ST, Yang LT. Hes1 regulates anagen initiation and hair follicle regeneration through modulation of hedgehog signaling. Stem Cells. 2020;38(2):301–14.
39. Aoi N, Inoue K, Chikanishi T, Fujiki R, Yamamoto H, Kato H, et al. 1α,25-dihydroxyvitamin D3 modulates the hair-inductive capacity of dermal

papilla cells: therapeutic potential for hair regeneration. Stem Cells Transl Med. 2012;1(8):615–26.
40. Lopez-Bergami P, Lau E, Ronai Z. Emerging roles of ATF2 and the dynamic AP1 network in cancer. Nat Rev Cancer. 2010;10(1):65–76.
41. Hernandez JM, Floyd DH, Weilbaecher KN, Green PL, Boris-Lawrie K. Multiple facets of jund gene expression are atypical among AP-1 family members. Oncogene. 2008;27(35):4757–67.
42. Bejjani F, Evanno E, Zibara K, Piechaczyk M, Jariel-Encontre I. The AP-1 transcriptional complex: local switch or remote command? Biochim Biophys Acta Rev Cancer. 2019;1872(1):11–23.
43. Fan F, Bashari MH, Morelli E, Tonon G, Malvestiti S, Vallet S, et al. The AP-1 transcription factor JunB is essential for multiple myeloma cell proliferation and drug resistance in the bone marrow microenvironment. Leukemia. 2017;31(7):1570–81.
44. Maity P, Singh K, Krug L, Koroma A, Hainzl A, Bloch W, et al. Persistent JunB activation in fibroblasts disrupts stem cell niche interactions enforcing skin aging. Cell Rep. 2021;36(9):109634.
45. Hsieh T, Sasaki D, Taira N, Chien H, Sarkar S, Seto Y, et al. JunB is critical for survival of T helper cells. Front Immunol. 2022;13:901030.
46. Donet E, Bayo P, Calvo E, Labrie F, Pérez P. Identification of novel glucocorticoid receptor-regulated genes involved in epidermal homeostasis and hair follicle differentiation. J Steroid Biochem Mol Biol. 2008;108(1–2):8–16.
47. Gago-Lopez N, Mellor LF, Megías D, Martín-Serrano G, Izeta A, Jimenez F, et al. Role of bulge epidermal stem cells and TSLP signaling in psoriasis. EMBO Mol Med. 2019;11(11):e10697.
48. Hui T, Zheng Y, Yue C, Wang Y, Bai Z, Sun J, et al. Screening of cashmere fineness-related genes and their ceRNA network construction in cashmere goats. Sci Rep. 2021;11(1):21977.
49. Holland JD, Klaus A, Garratt AN, Birchmeier W. Wnt signaling in stem and cancer stem cells. Curr Opin Cell Biol. 2013;25(2):254–64.
50. Rishikaysh P, Dev K, Diaz D, Qureshi WM, Filip S, Mokry J. Signaling involved in hair follicle morphogenesis and development. Int J Mol Sci. 2014;15(1):1647–70.
51. Tang T, Guo C, Xia T, Zhang R, Zen K, Pan Y, et al. LncCCAT1 promotes breast cancer stem cell function through activating Wnt/β-catenin signaling. Theranostics. 2019;9(24):7384–402.
52. Yi F, Pereira L, Hoffman JA, Shy BR, Yuen CM, Liu DR, et al. Opposing effects of Tcf3 and Tcf1 control Wnt stimulation of embryonic stem cell self-renewal. Nat Cell Biol. 2011;13(7):762–70.
53. Robinson KF, Narasipura SD, Wallace J, Ritz EM, Al-Harthi L. β-Catenin and TCFs/LEF signaling discordantly regulate IL-6 expression in astrocytes. Cell Commun Signal. 2020;18(1):93.
54. Tsai SY, Sennett R, Rezza A, Clavel C, Grisanti L, Zemla R, et al. Wnt/β-catenin signaling in dermal condensates is required for hair follicle formation. Dev Biol. 2014;385(2):179–88.
55. Sunkara RR, Mehta D, Sarate RM, Waghmarey SK. BMP-AKT-GSK3β signaling restores hair follicle stem cells decrease associated with loss of Sfrp1. Stem Cells. 2022;40(9):802–17.

Publisher's Note